journal

*J. Am. Ceram. Soc.*, **89** [2] 515–518 (2006)
DOI: 10.1111/j.1551-2916.2005.00782.x


# Photocatalytic Activity of Ni 8 wt%-Doped $TiO_2$ Photocatalyst Synthesized by Mechanical Alloying Under Visible Light

Dong Hyun Kim† and Kyung Sub Lee

Division of Materials Science & Engineering, Hanyang University, Seoul 133-171, Korea

Yoon-Suk Kim and Yong-Chae Chung

Department of Ceramic Engineering, Hanyang University, Seoul 133-791, Korea

Sun-Jae Kim

Department of Nano Science and Technology/SAINT, Sejong University, Seoul 143-747, Korea

**Ni 8 wt%-doped titanium dioxide ($TiO_2$) was synthesized by mechanical alloying. The photocatalytic activity of Ni 8 wt%-doped $TiO_2$ powder was evaluated by measuring the visible light absorption ability by ultraviolet visible diffuse reflectance spectroscopy (UV/Vis-DRS) and photoluminescence (PL) spectroscopy. Ni 8 wt%-doped $TiO_2$ powders had only a rutile phase and spherical particles with an average grain size of less than 10 nm. The UV/Vis-DRS analysis showed that the UV absorption for the Ni 8 wt%-doped $TiO_2$ powder moved to a longer wavelength and the photoreactivity was rapidly enhanced. And PL results revealed that the new absorption was believed to be induced by localization of the trapping level near the valance band or conduction band. Moreover, Ni 8 wt%-doped $TiO_2$ had a high reaction activity for decomposition of 4-chlorophenol in aqueous solution under UV and visible light. To obtain the electronic structure of Ni-doped $TiO_2$, we have performed *ab initio* pseudopotential plane wave methods based on the density functional theory. The band gap of Ni-doped $TiO_2$ narrowed more than pure $TiO_2$. These results agree with the experimentally observed phenomenon.**

## I. Introduction

Titanium dioxide ($TiO_2$) has been receiving considerable attention because of its chemical stability, low cost, and nontoxicity. However, $TiO_2$ is only excited by UV light so that the efficiency of solar light is very low.[1–3] Therefore, current research has sought to improve the photocatalystic properties of $TiO_2$ by doping with metals or oxides.[4–6] However, the photoactivity of the cation-doped $TiO_2$ decreased even in the UV region. This is because the doped materials show an increase in the carrier-recombination centers and are unstable at high temperature.[7] Moreover, the absorption spectra of anion-doped $TiO_2$ in the visible light region are comparatively in small range of about 400 nm.[8] In our previous paper,[9] nanocrystalline Fe-doped rutile $TiO_2$ synthesized by mechanical alloying (MA) and homogeneous precipitation process at low temperatures (HPPLT) exhibited an absorption threshold in the range 427–496 nm. However, the visible light absorption decreased when the Fe content exceeded 4.57 wt%. In this study, nanocrystalline $TiO_2$ powders doped with Ni 8 wt% were synthesized by MA and HPPLT methods. The photocatalytic activities of the powders were characterized by measuring reaction ability under visible light, and the detailed microstructural characteristics and electronic structures of the Ni 8 wt%-doped $TiO_2$ catalyst system were investigated.

## II. Experimental Procedure

Nanocrystalline Ni 8 wt%-doped $TiO_2$ powders were prepared by MA and HPPLT. To obtain a better doping effect, HPPLT rutile powder was selected as the starting powder for MA, instead of a stable $TiO_2$ phase. And to obtain the meta-stable powder, a $TiO(OH)_2$ precipitate slurry was first prepared from $TiOCl_2$ using the HPPLT process and then the solution was filtered using distilled water. The detailed HPPLT process has been reported elsewhere.[9] The filtered precipitates were dried at 60°C for 12 h to obtain the dried $TiO_2$ powder. The dried powder was mechanically alloyed for 14 h by a planetary ball mill (Fritsch, Kastl-Utzenhofen, Germany, P-5) with Ni powders (Kojundo Chem. Co., Ltd., 99.9%). The Ni contents varied from 4 to 10 wt%. The ball-milling speed was 150 rpm, and the ball to powder weight ratio was 15:1. The structural evaluation of the alloying process and nanocrystallization process including grain size determination were performed by high-resolution XRD (HRXRD, $Cu_{K\alpha}$, Bruker, Rheinstetten, Germany, DA8 Discover) and by high-resolution transmission electron microscopy (HRTEM, 400 KV, JEM 4010, Tokyo, Japan). The characteristics of visible light reaction were investigated by ultra violet visible diffuse reflectance spectroscopy (UV/Vis-DRS) (DRS Perkin–Elmer, Wellesley, MA) and photoluminescence (PL) (PC-1 Photon counting Spectroflourmeter, ISS, Champaign, IL). The specific surface area was measured by the BET method. The electronic structures of 8 wt%-doped $TiO_2$ were determined by pseudopotential plane wave calculations based on the density functional theory within the generalized gradient approximation (GGA) scheme,[10] as implemented in the Viennna *ab initio* simulation package.[11,12] Wave functions were expanded in terms of the plane wave basis set with a cutoff energy of 340 eV. The **k**-space integration was replaced by a summation over $(4 \times 4 \times 6)$ Monkhorst–Pack **k** points containing the Γ point. All atoms in the supercell were relaxed until the remaining forces became smaller than 0.01 eV/Å. The oxidation state of substituted Ni ion was verified with X-ray photoelectron spectroscopy (XPS, JEOL).

## III. Results and Discussion

Figure 1 shows the normal XRD patterns of the HPPLT powder, commercial P-25 powder (Degussa Co.), the Ni 8 wt%-

P. Gouma—contributing editor

Manuscript No. 20251. Received March 2, 2005; approved September 12, 2005.
Supported by the Energy Technology Academy Promotion and the Brain Korea 21 Project.
†Author to whom correspondence should be addressed. e-mail: dhk@ihanyang.ac.kr

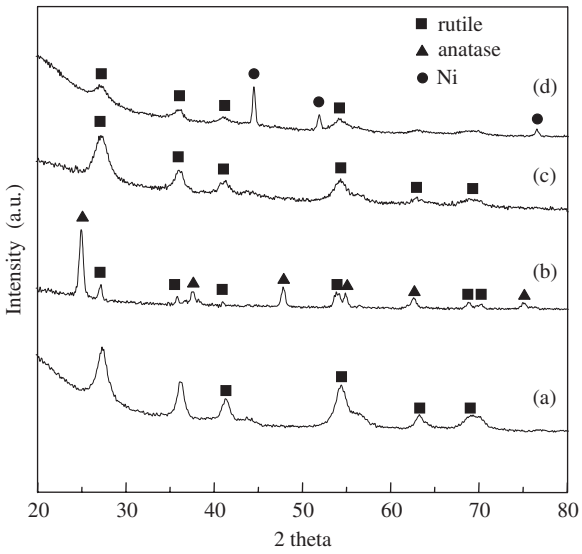


**Fig. 1.** XRD patterns of $TiO_2$ powders: (a) homogeneous precipitation process at low temperatures powder, (b) P-25, (c) Ni 8 wt%-doped $TiO_2$, (d) Ni 10 wt%-doped $TiO_2$.

doped powder, and Ni 10 wt%-doped powder. It can be seen that the Ni 8 wt%-doped powder and the HPPLT powders have only a rutile phase, whereas the P-25 powder is a mixture of the rutile and the anatase phase. And, in case of Ni 8 wt%-doped powder, Ni element was not detected. It is thought that the Ni element was dissolved in the rutile $TiO_2$ matrix. However, when Ni content higher than 8 wt% was added, the Ni element appeared at around 44.5° and 51.5° of the diffraction angle (2θ). The Ni 8 wt%-doped powder and HPPLT powder peaks broadened, but the P-25 peak was sharp. The HPPLT powder exhibited a peak-broadening characteristic of nanocrystalline materials. In the case of Ni 8 wt%-doped powder, the peak broadening indicates a refinement of the average crystallite size and an increase in the internal strain by mechanical deformation during ball milling. Applying the Debye–Scherrer formula[13] and the full-width at half-maximum to the (110) reflection, typical values of crystallite sizes have been calculated to be in the range of 5–15 nm for the Ni 8 wt%-doped powder and 30–40 nm for the commercial P-25 and 35–50 nm for the HPPLT rutile $TiO_2$ powder. They agree with the sizes determined from TEMs. Moreover, a diffraction peak for elemental Ni was detected when the content of Ni exceeded 8 wt%.

HRTEM analyses were carried out to observe the morphologies of the alloyed powders and to locate the position of Ni within the mechanically alloyed powders. Figure 2 shows the HRTEM micrographs of the Ni 8 wt%-doped powders and the HPPLT rutile powder. Figure 2(a) shows that the 8 wt% Ni-doped powder consisted of spherical particles with an average grain size of less than 10 nm. The HPPLT rutile powders had a chestnut bur shape with a size of 200–300 nm (Fig. 2(c)), in which the primary acicular particles were coagulated. The electron diffraction pattern of the Ni-doped powder is shown in Fig. 2(b). Ring patterns for (110), (101), and (200) planes of the rutile phase were observed with the lattice, which had slightly increased on Ni doping. However, Ni element patterns were not detected. This suggests that doping occurred by the complete dissolution of Ni in the rutile $TiO_2$ matrix. SEM analyses with energy-dispersive spectrometry were performed to follow the atomic distribution with milling time, and the results are shown in Fig. 3 and Table I. It is confirmed that Ni was uniformly distributed in the powder, and the Ni composition agrees with the nominal value.

BET analyses show that the Ni-doped powder has a larger surface area (234 $m^2/g$) than the P-25 powder and HPPLT powder (about 50 and 150 $m^2/g$). Consequently, it can be expected

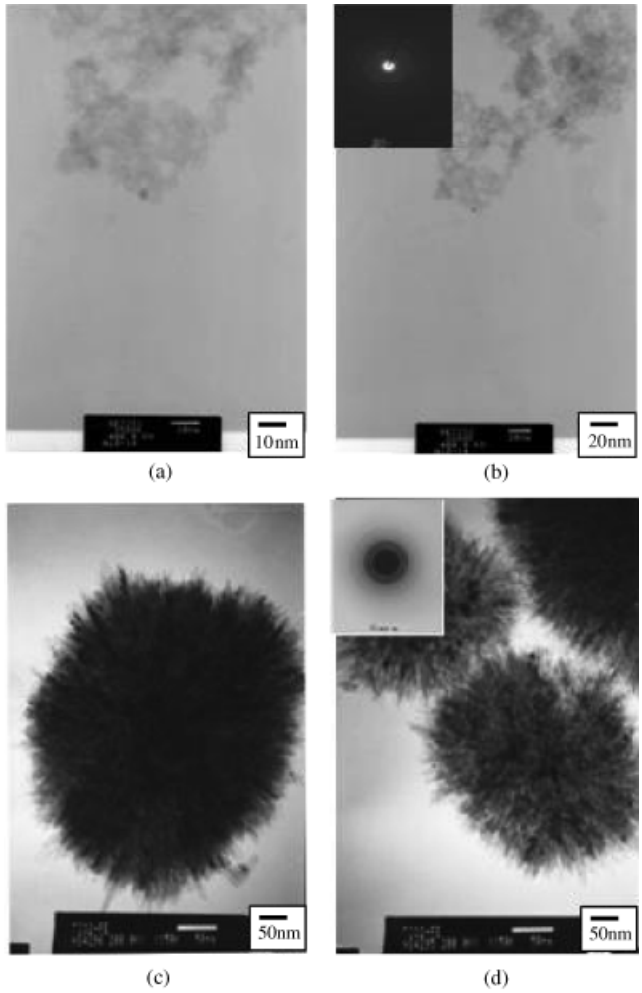


**Fig. 2.** High-resolution transmission electron microscopy micrographs of a mechanically alloyed $TiO_2$ powder and P-25 (a) Ni 8 wt%-doped $TiO_2$, (b) electron diffraction pattern of mechanical alloyed $TiO_2$, (c) homogeneous precipitation process at low temperatures (HPPLT) rutile $TiO_2$, (d) electron diffraction pattern of HPPLT rutile $TiO_2$.

that the photocatalytic activity of the Ni 8 wt%-doped $TiO_2$ powder will be higher than that of the P-25 powder from the viewpoint of the grain size.

Figure 4 shows the results of diffuse reflectance spectra of the HPPLT, the Ni 8 wt%-doped powder, and the P-25 powder. From Fig. 4, it can be seen that Ni 8 wt%-doped powder showed the greatest wavelength shift and longest wavelength as com-

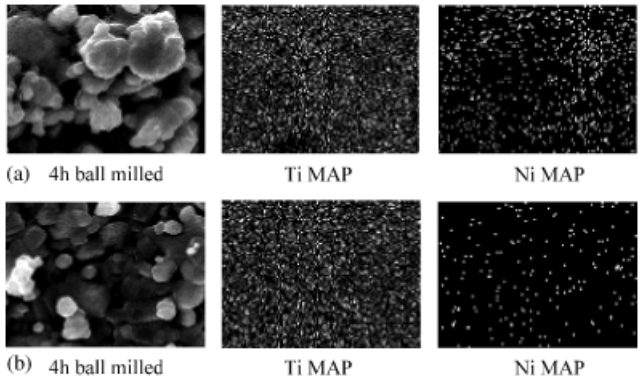


**Fig. 3.** SEM micrographs and energy dispersive spectroscopy images showing cross-sections of Ni 8 wt%-doped $TiO_2$ (a) for 4 h milling and (b) for 14 h milling.

**Table I. Quantitative Analysis Result for Ni 8 wt%-Doped $TiO_2$**

| Spectrum | O | Ti | Ni | Total |
|---|---|---|---|---|
| 1 | 14.51 | 77.90 | 7.59 | 100.00 |
| 2 | 18.41 | 73.97 | 7.62 | 100.00 |
| Max. | 18.41 | 77.90 | 7.52 | |
| Min. | 14.51 | 73.97 | 7.69 | |

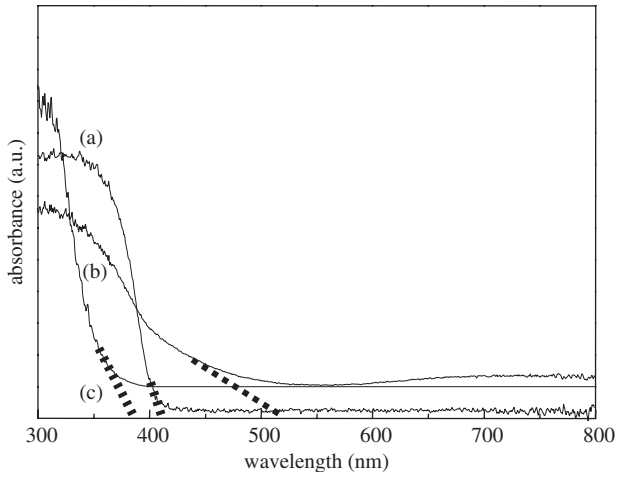


**Fig. 4.** UV/Vis-DRS data: (a) homogeneous precipitation process at low temperatures powder, (b) Ni 8 wt%-doped $TiO_2$, (c) P-25.

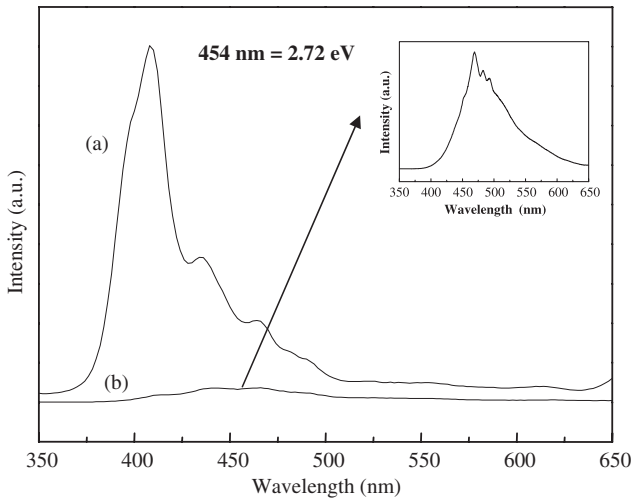


**Fig. 5.** Photoluminescence data: (a) homogeneous precipitation process at low temperatures powder, (b) Ni 8 wt%-doped $TiO_2$.

pared with other powders. Moreover, it is interesting to notice that the Ni 8 wt%-doped powder showed photoabsorption in the visible light region (wavelength = 480–500 nm), but the photoabsorption intensity was weak. This suggests that the Ni 8 wt%-doped $TiO_2$ has the ability to respond to the wavelength of the visible light region.[14] The most probable mechanism of the Ni 8 wt%-doped powder's red shift may be due to the localized trapping level within the rutile $TiO_2$ band gap by Ni doping during ball milling.

To locate the position of the additional energy level within the band gap of rutile $TiO_2$, PL spectra of the powders are shown in Fig. 5. The HPPLT powder showed an emission peak at around 408 nm (3.03 eV), while Ni 8 wt%-doped powders showed an

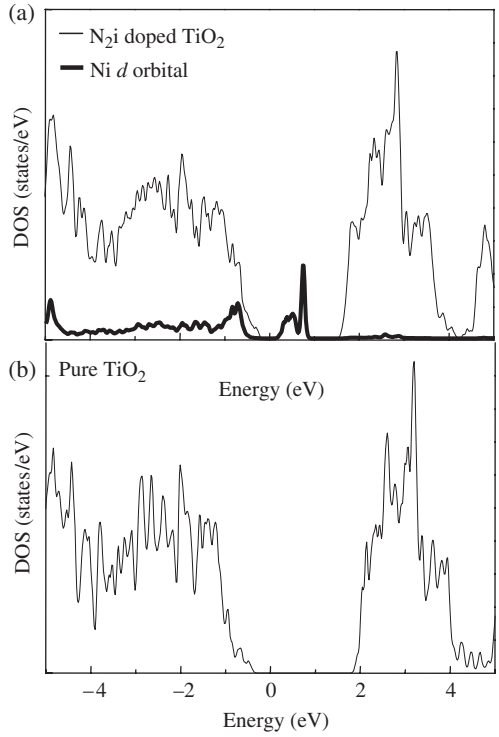


**Fig. 6.** Density of states of Ni 8 wt%-doped $TiO_2$ (a) homogeneous precipitation process at low temperatures powder, and (b) Ni 8 wt%-doped $TiO_2$.

emission peak at around 457 nm (2.71 eV). Addition of Ni led to a shift of the luminescence spectrum toward a longer wavelength region. A broad PL spectrum was observed in the visible region with a wide spectral width for the Ni 8 wt%-doped $TiO_2$, but the intensity was decreased by doping. The decrease of luminescence intensity, upon doping, may be due to the localization of the Ni trapping level in the rutile $TiO_2$ band gap.

To confirm the experimental result, the electronic structure was calculated by the *ab initio* band theory using the supercell approach. We adopted the eight unit cells of rutile $TiO_2$, where a Ti is replaced with Ni. A 48-atom supercell, therefore, was used to describe 6.25% Ni-doped $TiO_2$. In the pure rutile $TiO_2$, the band gap is located at a Γ point with a value of 2.5 eV. The simulated band gap is generally small to compare with the experimentally obtained band gap, because of the well-known in-

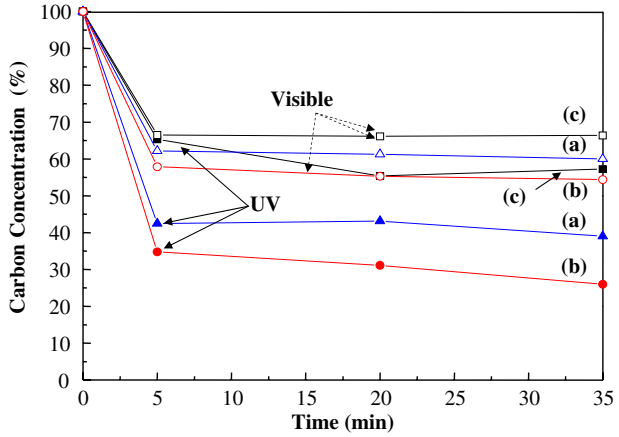


**Fig. 7.** Photocatalytic decomposition of 4-chrolophenol using various $TiO_2$ powders: (a) homogeneous precipitation process at low temperatures powder, (b) Ni-doped $TiO_2$, and (c) P-25.

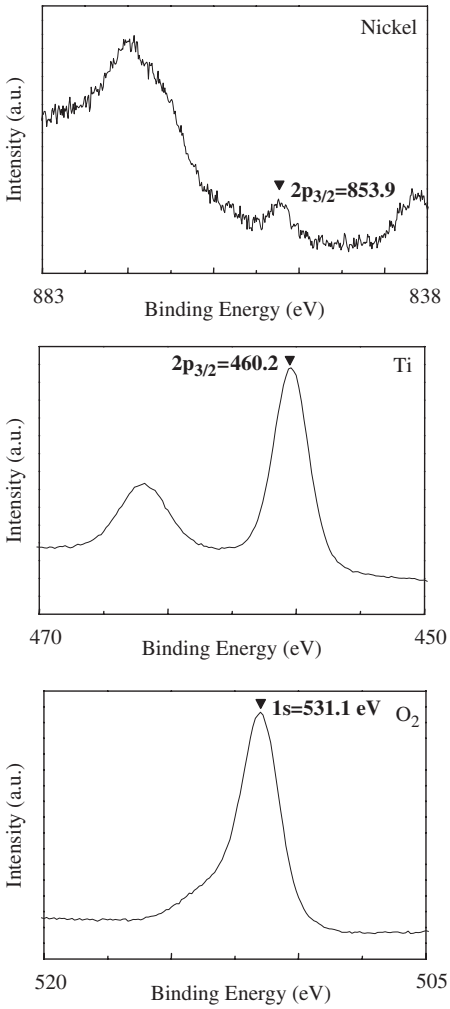


**Fig. 8.** X-ray photoemission spectroscopy spectra of Ni, O, and Ti on the surface of Ni 8 wt%-doped $TiO_2$ powder.

adequacy of the local density approximation[15] and the GGA.[16] As shown in Fig. 6, new absorption bands appeared within the band gap as an impurity energy level. The impurity states were related to 3*d* states of Ni transition metal. As they were partially occupied, the excited *d*-state electron could emit the photon that had a wavelength longer than UV. These results agree with UV/Vis-DRS and PL spectra.

The photocatalytic reaction abilities of the Ni 8 wt%-doped $TiO_2$ powder under UV and visible light irradiation were evaluated by measuring the decomposition of 4-chlorophenol, and the results are shown in Fig. 7. Under UV and visible light irradiation, the reaction activity of Ni 8 wt%-doped $TiO_2$ was about two times higher than that of P-25 and HPPLT powders. It is very important that we have synthesized a new $TiO_2$ powder that shows a photocatalytic reaction under a visible light range.

To investigate the Ni states in the Ni 8 wt%-doped $TiO_2$ powder, Ni $2p_{3/2}$ levels were measured by XPS, as shown in Fig. 8. The XPS result revealed that the oxidation state of Ni substituted into the $TiO_2$ lattice was Ni.

## IV. Conclusion

Nanocrystalline Ni 8 wt%-doped $TiO_2$ powders could be synthesized by MA and HPPLT. HRTEM and energy dispersive spectroscopy investigation verified that the added Ni atoms were dissolved in the rutile $TiO_2$ lattice with an average grain size of less than 10 nm. The UV/Vis-DRS absorption showed that the nano-sized Ni 8 wt%-doped powder had a higher wavelength range (480–500 nm) than the commercial P-25 powder and the HPPLT powder (380–400 nm). The PL spectrum of Ni 8 wt%-doped $TiO_2$ showed a shift in the emission peak toward the longer wavelength region, confirming a decrease in the band gap (2.72 eV). The electronic structure analysis using *ab initio* band calculations revealed band gap narrowing because of the formation of the impurity energy levels. And Ni 8 wt%-doped $TiO_2$ had a high reaction activity for decomposition of 4-chlorophenol in an aqueous solution under UV and visible light.

## References

[1]W. Choi, A. Termin, and M. R. Hoffmann, "Flux-Matching Conditions at $TiO_2$ Photoelectrodes: Is Interfacial Electron Transfer to $O_2$ Pare-Limiting in the $TiO_2$-Catalyzed Photochemistry Degradation of Organics?," *J. Phys. Chem.*, **98**, 13369 (1994).

[2]T. Morikawa, R. Asahi, T. Ohwaki, A. Aoki, and Y. Taga, "Band Gap Narrowing of Titanium Dioxide by Nitrogen Doping," *Jpn. T. Appl. Phys.*, **40**, Part 2, L561 (2001).

[3]H. E. Chao, Y. U. Yun, H. U. Xingfang, and A. Larbot, "Effect of Silver Doping on the Phase Transformation and Grain Growth of Sol-Gel Titania Powder," *J. Eur. Ceram. Soc.*, **23**, 1457–64 (2003).

[4]D. Madare, M. Tasca, M. Delibas, and G. I. Rusu, "On the Structural Properties and Optical Transmittance of $TiO_2$ r.f. Sputtered Thin Film," *Appl. Surf. Sci.*, **156**, 200 (2000).

[5]M. M. Rahman, K. M. Krishna, T. Soga, T. Jimbo, and M. Umeno, "Optical Properties and X-Ray Photoelectron Spectroscopic Study of Pure and Pb-Doped $TiO_2$ Thin Film," *J. Phys. Chem. Solids*, **60**, 201 (1999).

[6]K. M. Krishna, M. Mosaddeq-ur-Rahman, T. Miki, K. M. Krishna, T. Soga, K. Igarashi, S. Tanemura, and M. Umeno, "Optical Properties of Pb Doped $TiO_2$ Nanocrystalline Thin Film: A Photoluminescence Spectroscopic Study," *Appl. Surf. Sci.*, **113/114**, 149 (1997).

[7]T. Umebayashi, T. Yamaki, H. Itoh, and K. Asai, "Band Gap Narrowing of Titanium Dioxide by Sulfur Doping," *Appl. Phys. Lett.*, **81** [3] 454.

[8]T. Ohno, M. Akiyoshi, T. Umebayashi, K. Asai, T. Mitsui, and M. Matsumura, "Preparation of S-Doped $TiO_2$ Photocatalysts and Their Photocatalytic Activities Under Visible Light," *Appl. Catal. A: General*, **65**, 115–21 (2004).

[9]D. H. Kim, H. S. Hong, S. J. Kim, J. S. Jong, and K. S. Lee, "Photocatalytic Behaviors and Structural Characterization of Nanocrystalline Fe-Doped $TiO_2$ Synthesized by Mechanical Allying," *J. Alloys Compd.*, **375**, 259–264 (2004).

[10]J. P. Perdew, J. A. Chevary, S. H. Vosko, K. A. Jackson, M. R. Pederson, D. J. Singh, and C. Fiolhais, "Atoms, Molecules, Solids, and Surfaces: Applications of the Generalized Gradient Approximation for Exchange and Correlation," *Phys. Rev. B*, **46**, 6671 (1992).

[11]G. Kresse and J. Furthmüller. Vienna Ab initio Simulation Package (University of Wien, Vienna 2001)

[12]G. Kresse and J. Hafner, "Ab Initio Molecular Dynamics for Open-Shell Transition Metal," *Phys. Rev. B*, **47**, RC558 (1993).

[13]B. D. Culity, *Elements of X-Ray Diffraction*, 2nd edition, p. 101. Addison-Wesley, MA, 1978.

[14]Zou Zhigang, Ye Jinhua, and H. Arakawa, "Optical and Structural Properties of the $BaTa_{1-x}Nb_xO_4(0 \le x \le 1)$," *Solid State Commun.*, **119**, 471–5 (2001).

[15]J. P. Perdew, "Physical Content of the Exact Kohn–Sham Orbital Energies: Band Gap and Derivative Discontinuities," *Phys. Rev. Lett.*, **51**, 1884–7 (1983).

[16]C. Stampfl and C. G. Van de Wall, "Density-Functional Calculations for III–V Nitrides Using the Local-Density Approximation and the Generalized Gradient Approximation," *Phys. Rev. B*, **59**, 5521–35 (1999). □